

# Characterization of Finite Ground Coplanar Waveguide with Narrow Ground Planes

George E. Ponchak  
NASA Lewis Research Center  
MS 54/4  
21000 Brookpark Road  
Cleveland, Ohio 44135  
Phone: 216-433-3504  
Fax: 216-433-8705  
e-mail: caponch@popserve.lerc.nasa.gov

Emmanouil M. Tentzeris and Linda P.B. Katehi  
University of Michigan  
3240 EECS Building  
1301 Beal Avenue  
Ann Arbor, Michigan 48109-2122  
Phone: 313-647-1796  
Fax: 313-647-2106  
e-mail: katehi@eecs.umich.edu

---

## Abstract

*Coplanar waveguide with finite width ground planes is characterized through measurements, conformal mapping, and the Finite Difference Time Domain (FDTD) technique for the purpose of determining the optimum ground plane width. The attenuation and effective permittivity of the lines are related to its geometry. It is found that the characteristics of the Finite Ground Coplanar line (FGC) are not dependent on the ground plane width if it is greater than twice the center conductor width, but less than  $\lambda_d/8$ . In addition, electromagnetic field plots are presented which show for the first time that electric fields in the plane of the substrate terminate on the outer edge of the ground plane, and that the magnitude of these fields is related to the ground plane width.*

---

## Key words:

Microwave Transmission Lines, Coplanar Waveguides, Propagation Characteristics.

---

## 1. Introduction

Finite Ground Coplanar waveguide (FGC) is being used more extensively in microwave and millimeter-wave integrated circuits<sup>1,2</sup> because it has several advantages over conventional

coplanar waveguide (CPW) with its semi-infinite ground planes. Novel circuit components that are not possible in CPW can be implemented in FGC<sup>3</sup>. Also, resonances that are established by the edges of the substrate and the package walls of CPW<sup>4,5</sup> can be eliminated by designing the ground plane width  $B$  shown in Figure 1 so that it is less than  $\lambda_d/4$  where  $\lambda_d$  is the wavelength in the dielectric substrate,  $\lambda_0/\sqrt{\epsilon_r}$ . Furthermore, it has been shown that if the ground plane is large compared to the other geometric parameters, the effective permittivity and the characteristic impedance of FGC is not a function of the ground plane width<sup>6-8</sup>.

The goal of circuit designers is to increase the circuit density. Therefore, the question that must be answered as to how small the



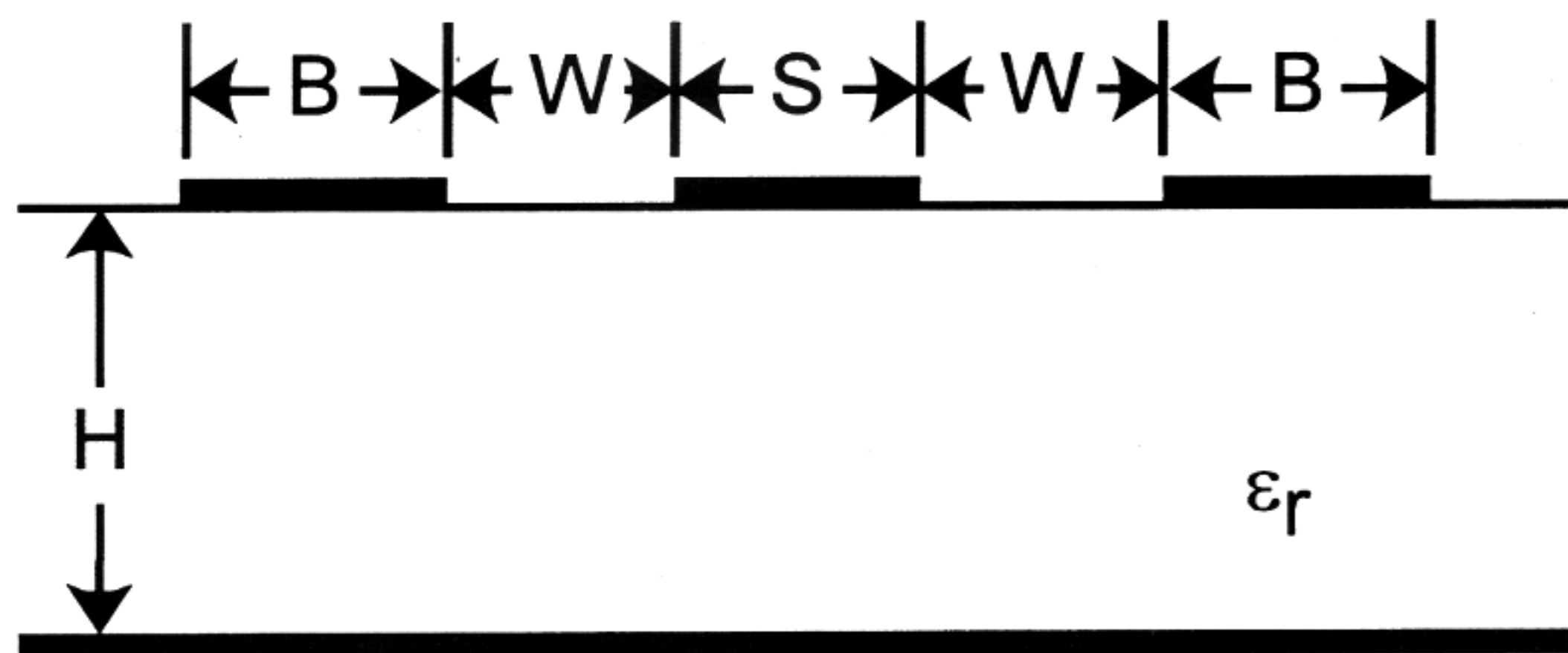


Figure 1. Coplanar waveguide with finite width ground planes (FGC).

ground plane width can be made while maintaining the desirable characteristics of low attenuation and dispersion. In this paper, measured attenuation and effective permittivity,  $\epsilon_{\text{eff}}$ , of FGC transmission lines is presented as a function of the ground plane width for values comparable to the strip and slot widths. In addition, conformal mapping is used to characterize the line, and the attenuation and the effective dielectric constant derived through this analysis is compared to the measured characteristics. Finally, the Finite Difference Time Domain (FDTD) analysis and the conformal mapping analysis are used to show for the first time the magnetic field distribution of this newly developed line and the existence of propagating power on the surface of the substrate (but outside the ground plane edges).

## 2. Measurement Technique

Finite ground coplanar lines with  $S=W=25\mu\text{m}$  and  $S=W=50\mu\text{m}$  and ground widths ranging from  $S$  to  $15S$  are fabricated on high resistivity silicon,  $\rho > 2500\Omega\text{-cm}$  and  $\epsilon_r=11.9$ , wafers of  $411\mu\text{m}$  thickness with a back side ground plane and  $1.3\mu\text{m}$  Au metallization. The attenuation and effective dielectric constant are measured from 1 to 110 GHz using a network analyzer, GGB Industries Picoprobes, and a TRL calibration technique<sup>9</sup> that employs four delay lines to cover the entire frequency range. To reduce errors, each set of measurements is repeated three times and the results are averaged.

## 3. Analysis

Although significant design data exists for conventional CPW, there is very little design procedures for the finite ground lines. Using conformal mapping, FGC can be transformed into a conventional coplanar waveguide geometry. First, magnetic walls are assumed to exist on the surface of the substrate where there are no metal strips. In addition, it is assumed that the substrate thickness is large enough that the lower ground plane may be eliminated.

Furthermore, realizing the symmetry of the transmission line for the coplanar waveguide mode, only the first quadrant of the transmission line is required. The conformal mapping is shown in Figure 2 where the  $w$  plane is related to the  $z$  plane by:

$$w(z) = z \sqrt{\frac{c^2 - b^2}{c^2 - z^2}} \quad (1)$$

This transformation maintains the parameter  $b$  between the two transmission lines. Thus, the finite ground coplanar line is transformed into the infinite ground CPW with:

$$\frac{a^{\text{CPW}}}{a^{\text{FGC}}} = \frac{S^{\text{CPW}}}{S^{\text{FGC}}} = \frac{k^{\text{CPW}}}{k^{\text{FGC}}} = \sqrt{\frac{1 - \left(\frac{1}{1+2B'k^{\text{FGC}}}\right)^2}{1 - \left(\frac{k^{\text{FGC}}}{1+2B'k^{\text{FGC}}}\right)^2}} \quad (2)$$

where  $k = S/(S+2W)$ ,  $B' = B/S^{\text{FGC}}$  is the normalized ground plane width, and the superscript indicates the transmission line type. After determining the equivalent CPW by conformal mapping, the propagation characteristics of the FGC are determined from closed form equations that account for finite metal thickness<sup>13</sup>.

For a rigorous, theoretical analysis of FGC, the FDTD method<sup>10</sup> is employed. The 2D Xiao-Vahldieck<sup>11</sup> collapsed-cell algorithm has been chosen due to its superior accuracy capability. In this implementation, the magnetic field components are shifted by half a discretization interval in space and time domain with respect to the electric field components.

For a homogeneous medium with a permittivity  $\epsilon$  and per-

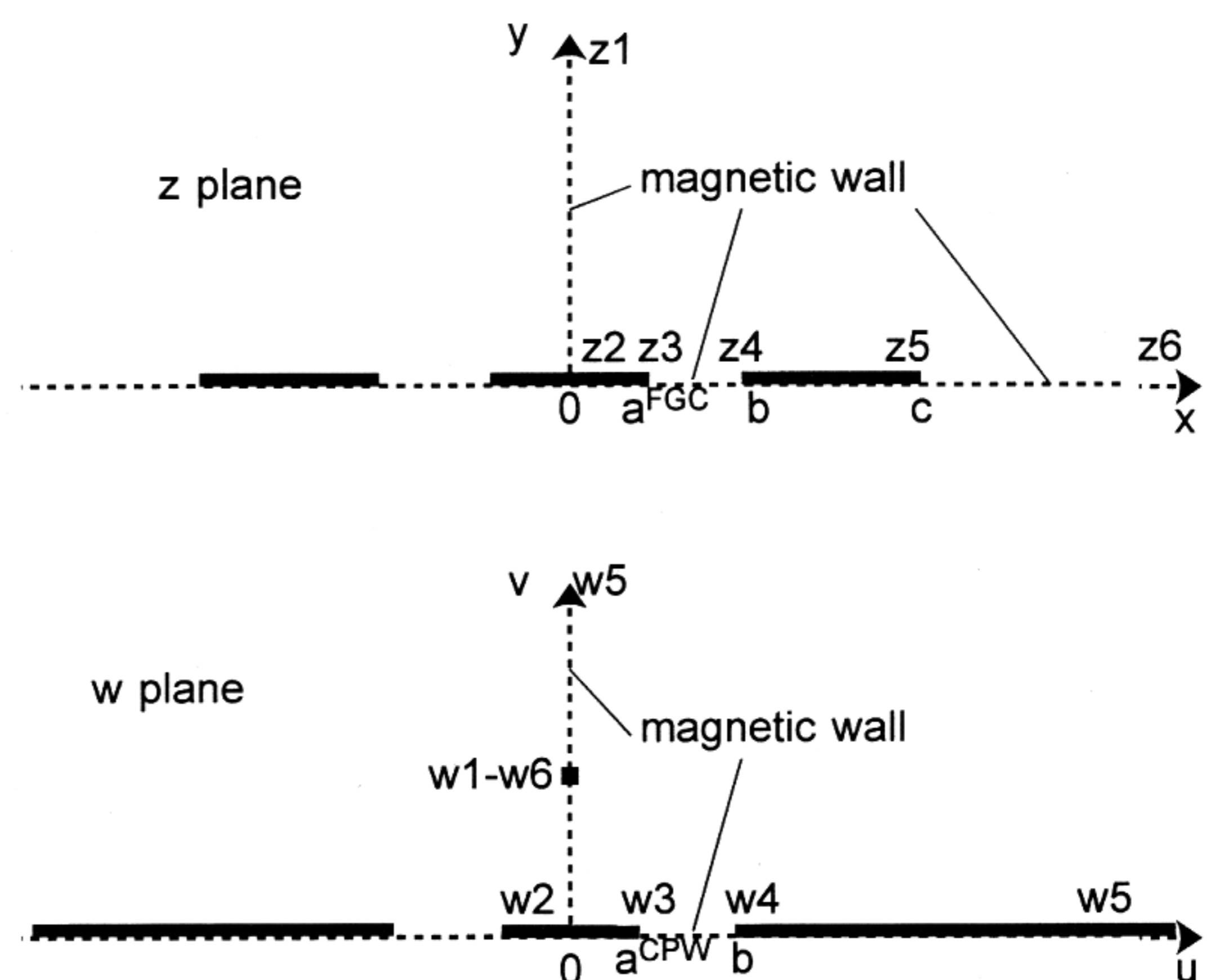


Figure 2. Conformal mapping of FGC into equivalent conventional CPW.



meability  $\mu$ , Maxwell's H-curl equation:  $\nabla \times \mathbf{H}' = \epsilon \frac{\partial \mathbf{E}'}{\partial \tau}$  may be written in the form of the following three scalar equations:

$$\frac{\partial H'_z}{\partial y} - \frac{\partial H'_y}{\partial z} = \epsilon \frac{\partial E'_x}{\partial \tau} \quad (3)$$

$$\frac{\partial H'_x}{\partial z} - \frac{\partial H'_z}{\partial x} = \epsilon \frac{\partial E'_y}{\partial \tau} \quad (4)$$

$$\frac{\partial H'_y}{\partial x} - \frac{\partial H'_x}{\partial y} = \epsilon \frac{\partial E'_z}{\partial \tau} \quad (5)$$

For the E-curl equation, three dual scalar equations are obtained.

Based on Reference<sup>11</sup>, the electric and the magnetic field components can be written as:

$$E'_x, E'_y, H'_z = [E_x(x,y,t), E_y(x,y,t), H_z(x,y,t)]je^{-j\beta z} \quad (6)$$

$$H'_x, H'_y, E'_z = [H_x(x,y,t), H_y(x,y,t), E_z(x,y,t)]e^{-j\beta z} \quad (7)$$

where  $\beta$  is the propagation constant. The factor  $j = 0+1j$  has been introduced in order to obtain a real-variable discretization process. Equations 3-5 can be written as:

$$\epsilon \frac{\partial E_x}{\partial \tau} = \frac{\partial H_z}{\partial y} + \beta H_y \quad (8)$$

$$\epsilon \frac{\partial E_y}{\partial \tau} = -\beta H_x - \frac{\partial H_z}{\partial x} \quad (9)$$

$$\epsilon \frac{\partial E_z}{\partial \tau} = \frac{\partial H_y}{\partial x} - \frac{\partial H_x}{\partial y} \quad (10)$$

and discretized by use of central differences for the approximation of the time and space derivatives.

The first step is to define a problem space of reasonable dimensions for computation. The dimensions of the Yee's cell for the simulations are chosen to be  $2.5\mu\text{m}$  for the direction parallel to the coplanar line and  $25\mu\text{m}$  for the normal direction. The time step is chosen to be  $7.45\text{ ps}$  to satisfy the Courant stability criterion. The first-order Mur's absorbing boundary condition<sup>12</sup> is applied to the top, left, and right boundaries of the problem computational space. The top absorber is placed at a distance equal to 15 times the dielectric thickness and the side absorbers at a distance equal to 7 times the gap of the coplanar line. A delta function with even (odd) symmetry is used for the excitation of the horizontal electric field across the gaps (even/odd coplanar-line mode). The propagation constant chosen for the simulations has the value 100.

## 4. Results and Discussion

The measured effective dielectric constant is shown in Figures 3(a) and 3(b) for lines with  $S$  and  $W$  of  $25$  and  $50\mu\text{m}$ , respectively. For both sets of lines, the effective permittivity varies by less than one percent as the normalized ground width varies from one to fifteen for low frequencies. This small variation is within the measurement error and supports the assumption of a magnetic wall along the surface of the unmetallized substrate. However, two lines behave differently at higher frequencies. For the line with the narrower strip and slot width, the line is nondispersive until the total line width approaches  $\lambda_d/2$ , and the lines with the wider strip and slot width become dispersive when the total line width approaches  $\lambda_d/4$ . This region of high dispersion is due to coupling to the parasitic microstrip mode which is stronger when  $H/(S+2W)$  is small<sup>14</sup>. Furthermore, when the total width of the line approaches  $\lambda_d/2$ , distinct resonances are established that substantially influence propagation. Results for wide lines above this limit are not presented in order to maintain clarity in the figures.

Figures 4(a) and 4(b) show the measured attenuation of the same finite ground lines. The attenuation decreases as the normalized ground width increases until it exceeds two. At which point, the attenuation as a function of  $B'$  saturates. This is shown by plotting the attenuation of finite ground lines normalized to the attenuation of infinite ground coplanar waveguide with the same strip and slot width as shown in Figure 5. Furthermore, at low frequencies, there is no measurable difference in attenuation as a function of the ground plane width. The na-

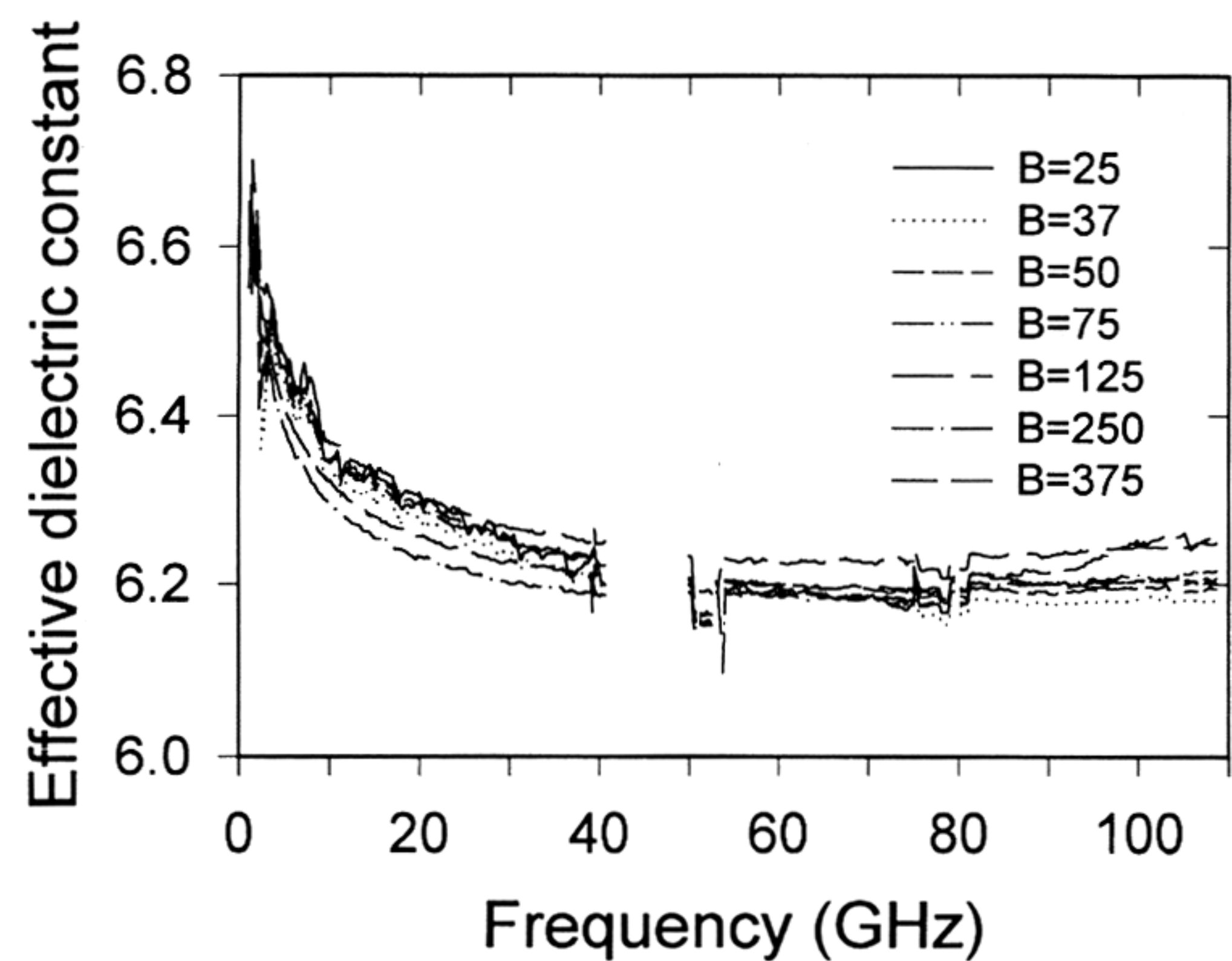


Figure 3(a). Measured effective dielectric constant of FGC as a function of frequency and ground plane width for  $S=W=25\mu\text{m}$ .



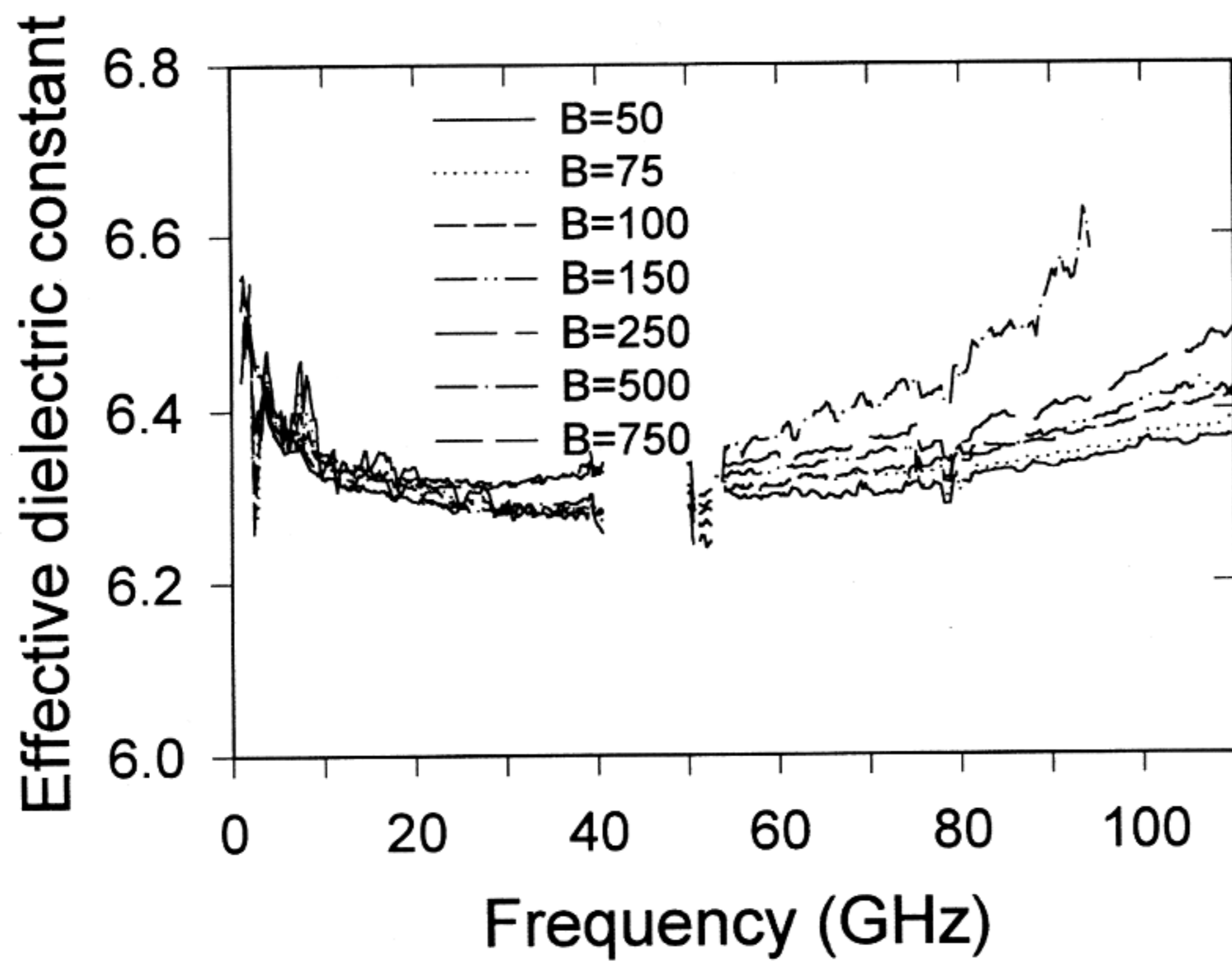


Figure 3(b). Measured effective dielectric constant of FGC as a function of frequency and ground plane width for  $S=W=50\ \mu\text{m}$ .

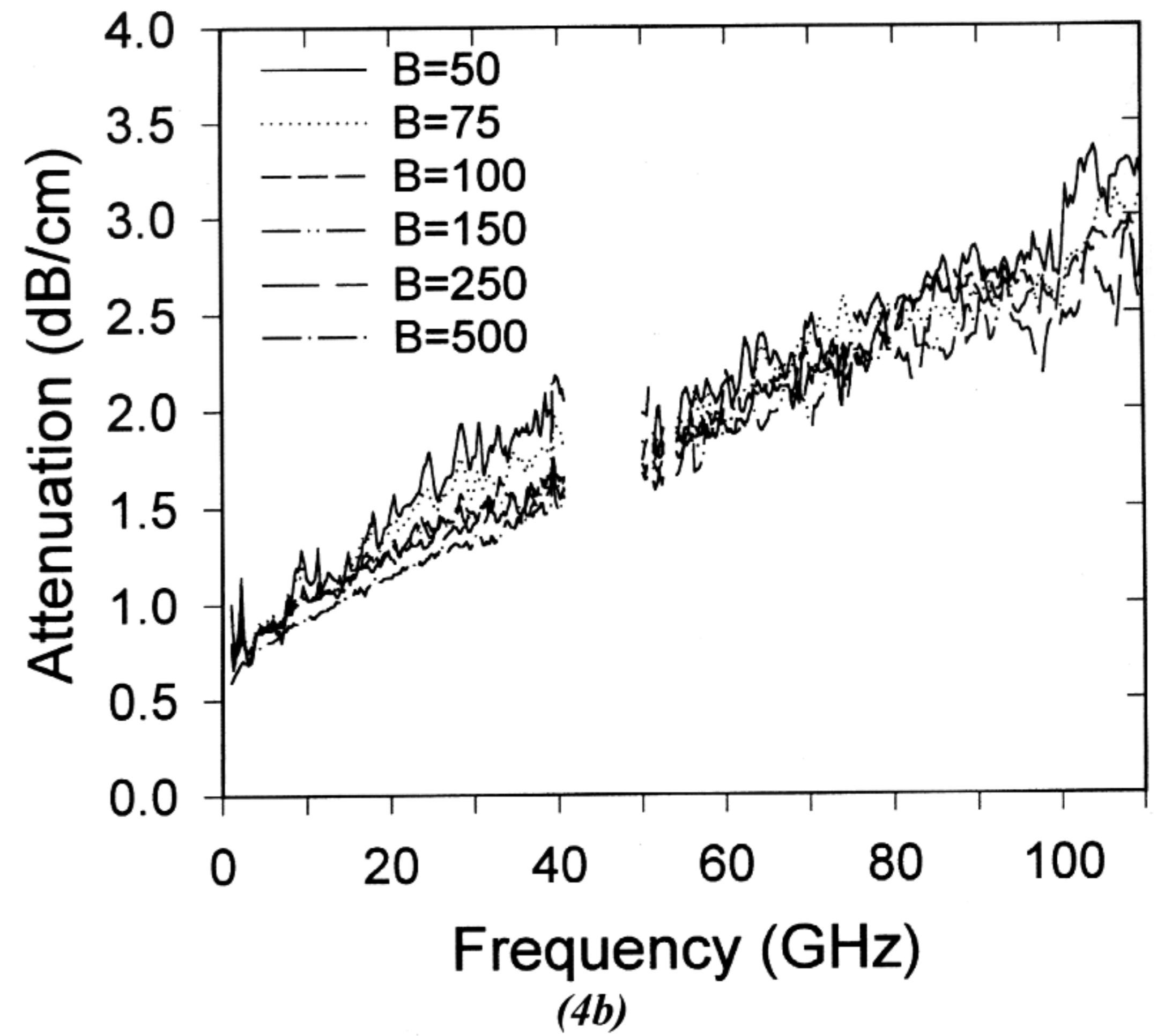


Figure 4(b). Measured attenuation of FGC as a function of frequency and ground plane width for  $S=W=50\ \mu\text{m}$ .

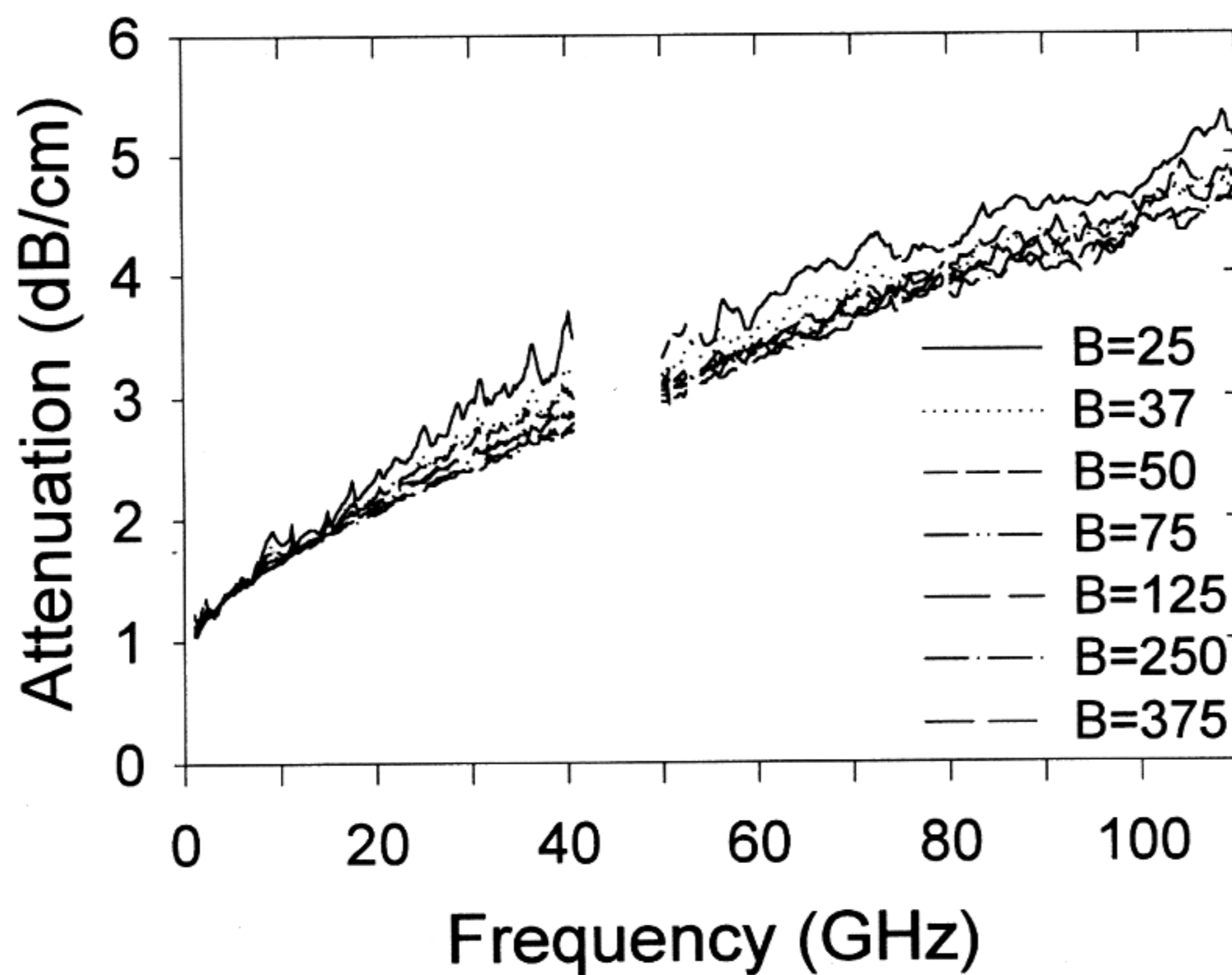


Figure 4(a). Measured attenuation of FGC as a function of frequency and ground plane width for  $S=W=25\ \mu\text{m}$ .

quency. It is found that the attenuation has a  $\sqrt{f}$  dependence for small values of  $B'$ . For  $B' > 2$ , the frequency dependence on the attenuation becomes  $f^{0.68}$ . This observation implies that the attenuation is conductor loss dominated for  $B' < 2$ , whereas for larger values of  $B'$ , dielectric and radiation losses become more noticeable. In the same way that the effective dielectric constant increases when the total width of the FGC approaches certain frequency limits, the measured attenuation also increases when this limit is reached. Furthermore, the attenuation increases dramatically when the total line width is greater than

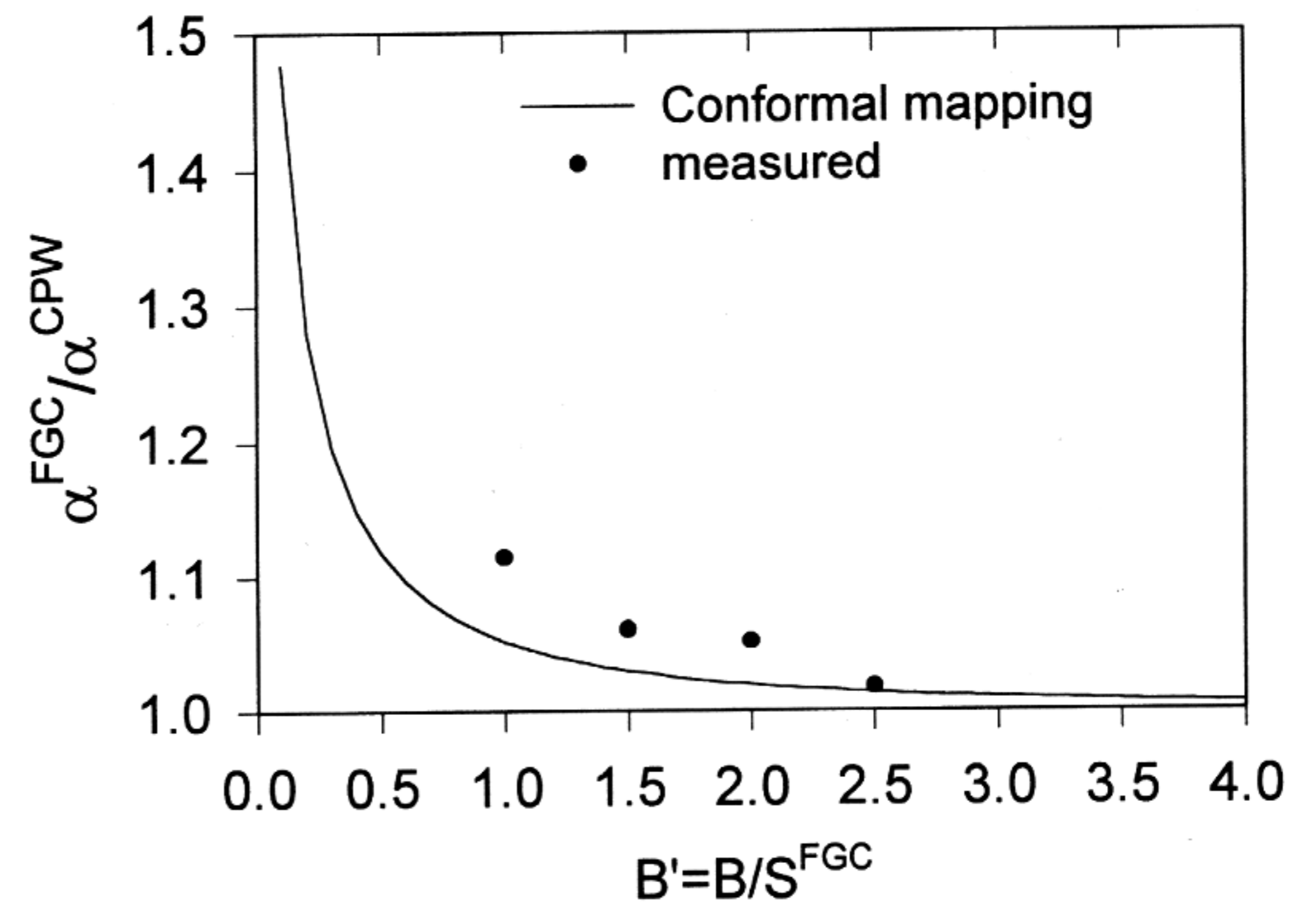


Figure 5. Attenuation of FGC with  $S=W=25\ \mu\text{m}$  normalized to the attenuation of conventional CPW with  $S=W=25\ \mu\text{m}$  as a function of the normalized ground plane width.

$\lambda_d/2$  and resonances are established. Again, data above this limit is not shown in Figures 4(a) and 4(b) to maintain clarity. Thus, the normalized ground width should be kept in a range between two and approximately  $\lambda_d/8$  to minimize conductor and radiation losses.

The critical design parameter in determining the character-



istic impedance of coplanar waveguide is the aspect ratio  $k$  defined by  $k = S/(S+2W)$ . From the conformal mapping analysis, the dependence of the ratio  $k^{CPW}/k^{FGC}$  on the FGC line geometry can be determined as shown in Figure 6. It is seen that for a normalized ground plane width greater than two, the FGC may be approximated by a conventional coplanar waveguide for most values of  $k^{FGC}$ . When the aspect ratio is greater than three, which is typical for most circuit designs, the reduction in the center strip conductor of an equivalent CPW line is less than ten percent.

An interesting feature of the FGC seen in the conformal mapping presented in this work that has not been previously presented is the mapping of the points 1 and 6 in the  $z$  plane to a finite position on the  $v$  axis of the  $w$  plane given by  $v = B \sqrt{(1 + k^{FGC} B') / k^{FGC} B'}$ . This point moves from infinity to zero as the ground width decreases from infinity to zero. For the CPW in the  $w$  plane, there is a magnetic wall along the  $v$  axis with magnetic fields encircling the center strip conductor that decay as  $v$  increases. The fields that cross the  $v$  axis between the points 1 and 2 of the  $w$  plane also encircle the center conductor of the  $z$  plane where they cross the  $y$  axis as  $H_x$  fields. At the same time, fields that cross the  $v$  axis between the points 6 and 5, map into  $H_y$  fields in the  $z$  plane that cross the  $x$  axis between the points 5 and 6. Thus, there is power that propagates along the FGC that is concentrated on the surface of the substrate, and the magnitude of this power is inversely dependent on the ground plane width. To better illustrate this, the magnetic field component  $H_y$  of the FGC calculated by the FDTD technique is plotted for lines with ground planes widths of 25 and 100  $\mu\text{m}$  in Figures 7(a) and 7(b), respectively. The field is approximately twice as strong for the narrower ground plane width, but it is also seen that the field decay from the

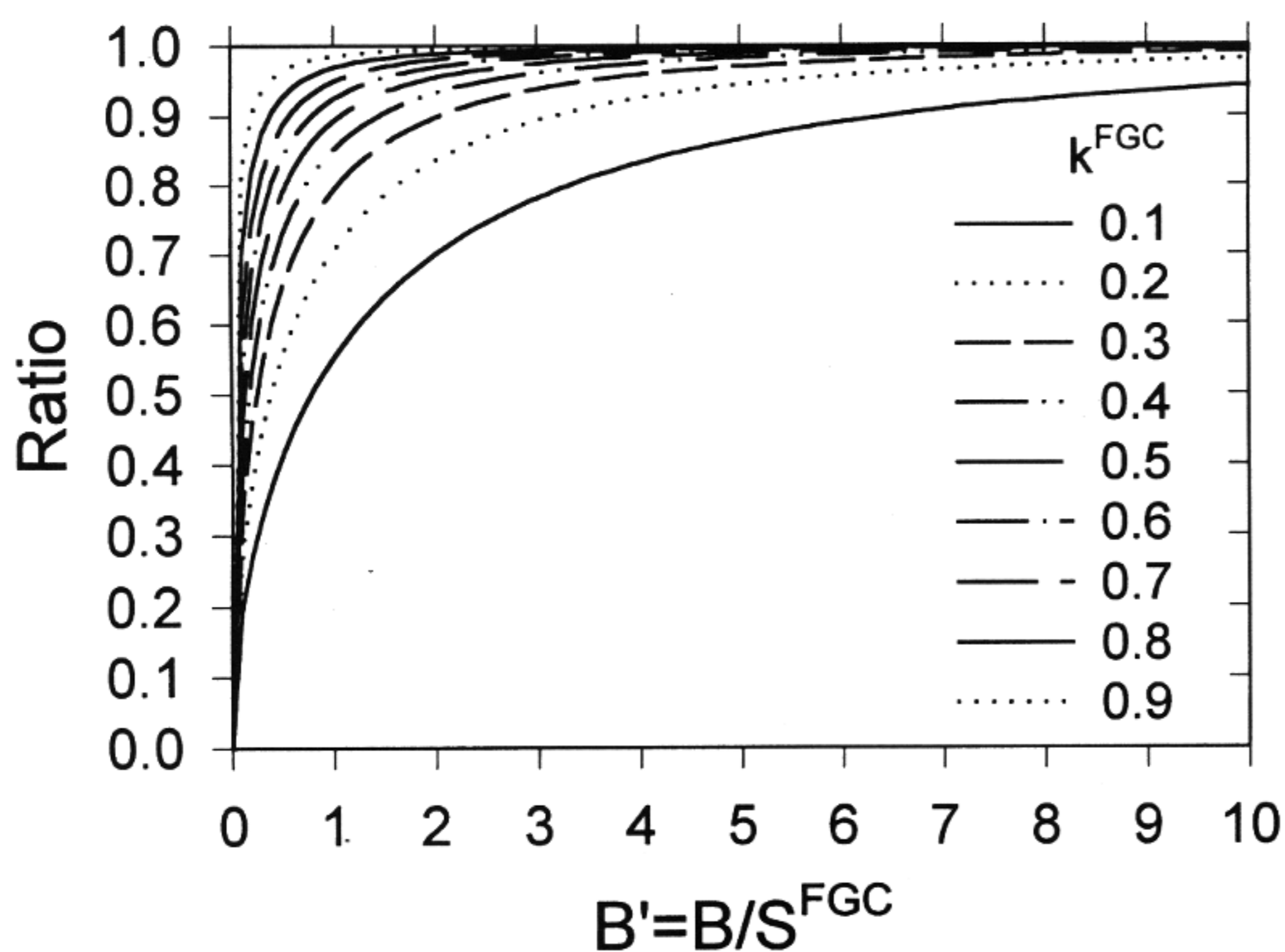


Figure 6. Ratio of the geometric parameters  $S$  and  $k$  of conventional CPW to FGC as a function of the normalized ground plane width and  $k$  of the FGC line.

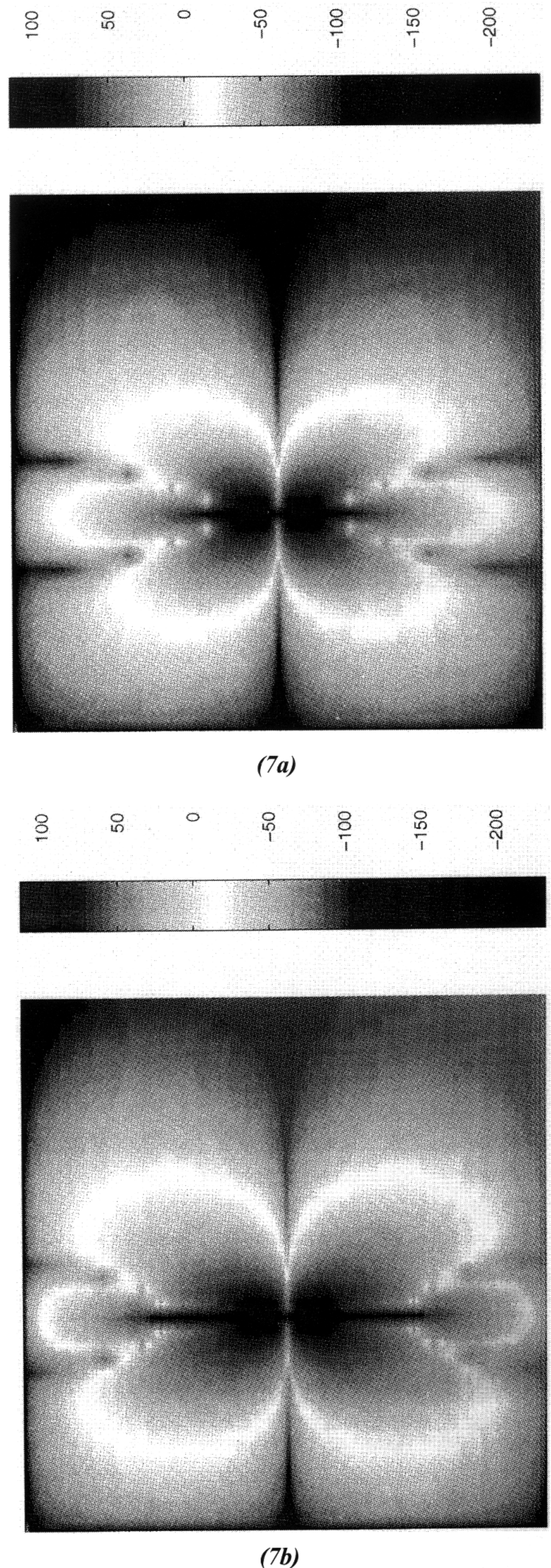


Figure 7.  $|H_y|$  of FGC with  $S = W = 25 \mu\text{m}$ ,  $H = 400 \mu\text{m}$ , and (a)  $B = 25 \mu\text{m}$  (b)  $B = 100 \mu\text{m}$ .



## 5. Conclusions

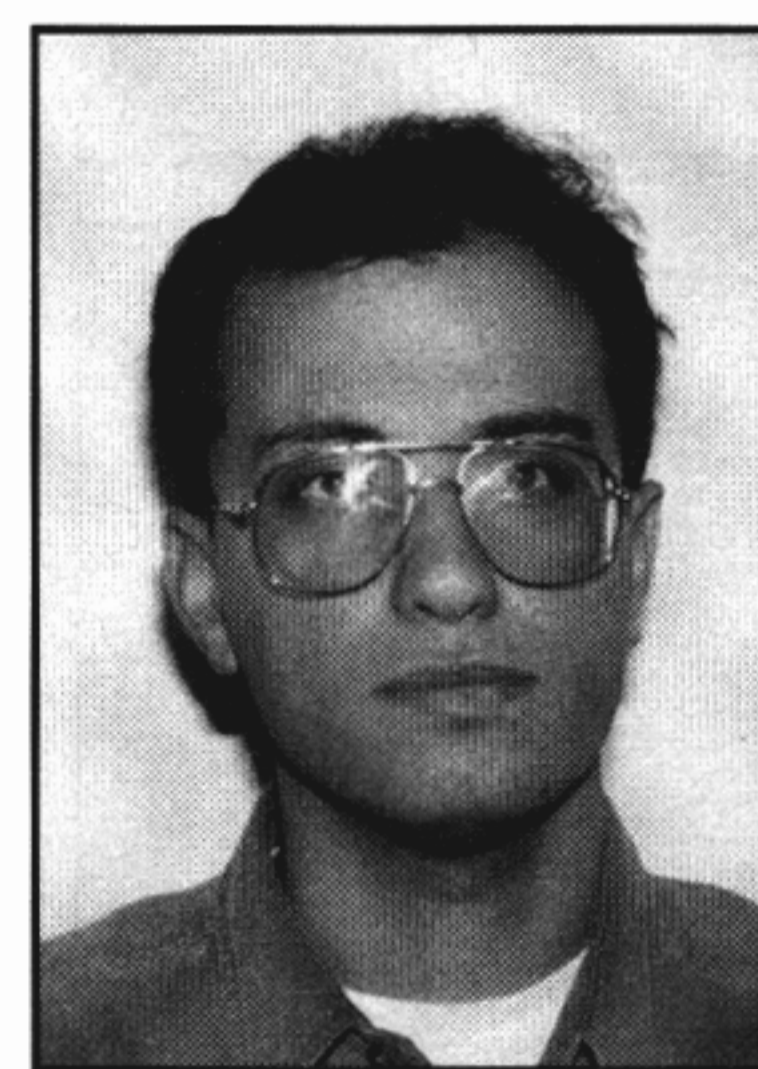
Finite width coplanar waveguide has been characterized for cases when the ground plane width is comparable to the center strip conductor width. It has been shown that the effective permittivity of the transmission line is independent of the ground plane width. In general, the attenuation is higher for a narrow ground plane width due to increased conductor loss; however, if the normalized ground plane width is greater than two, the difference in attenuation between FGC and CPW of the same  $S$  and  $W$  is very small. There is also an upper limit for the ground width of approximately  $\lambda_d/8$  to keep the radiation losses and dispersion small. The electromagnetic fields of finite ground line has been presented where it is shown that there is significant power on the surface of the substrate outside of the ground planes when the normalized ground plane width is small. However, the field decay from the center of the FGC is independent of the ground plane width. Thus, coplanar waveguide with a finite ground plane width as small as twice the center strip width may be used without adversely affecting the attenuation and permittivity of the lines. To eliminate coupling to parasitic modes, the total line width should be kept smaller than  $\lambda_d/4$ .

## References

1. C. Sinclair, "A Coplanar Waveguide 6-18 GHz Instantaneous Frequency Measurement Unit for Electronic Warfare Systems," *1994 IEEE International Microwave Symposium Dig.*, San Diego, CA, May 23-27, pp. 1767-1770, 1994.
2. F. Brauchler, S. Robertson, J. East, and Linda P. B. Katehi, "W-band Finite Ground Plane Coplanar (FGC) Line Circuit Elements," *1996 IEEE International Microwave Symposium Dig. San Francisco*, CA, June 17-21, pp. 1845-1848, 1996.
3. G. E. Ponchak, S. Robertson, F. Brauchler, J. East, and L. P. B. Katehi, "Finite Width Coplanar Waveguide for Microwave and Millimeter-Wave Integrated Circuits," *ISHM 1996 Proceedings International Symposium On Microelectronics*, Minneapolis, MN, Oct 8-10, pp. 517-521, 1996.
4. W. T. Lo, C. K. C. Tzuang, S. T. Peng, C. C. Tien, C. C. Chang, and J. W. Huang, "Resonant Phenomena in Conductor-Backed Coplanar Waveguides (CBCPW's)," *IEEE Trans. Microwave Theory and Techniques*, Vol. 41, No. 12, pp. 2099-2107, December 1993.
5. M. Yu, R. Vahldieck, and J. Huang, "Comparing Coax Launcher and Wafer Probe Excitation for 10 mil Conductor Backed CPW with Via Holes and Airbridges," *1993 IEEE International Microwave Symposium Dig.*, Atlanta, Georgia, June 14-18, pp. 705-708, 1993.
6. E. Mueller, "Measurement of the Effective Relative Permittivity of Unshielded Coplanar Waveguides," *Elect. Lett.*,

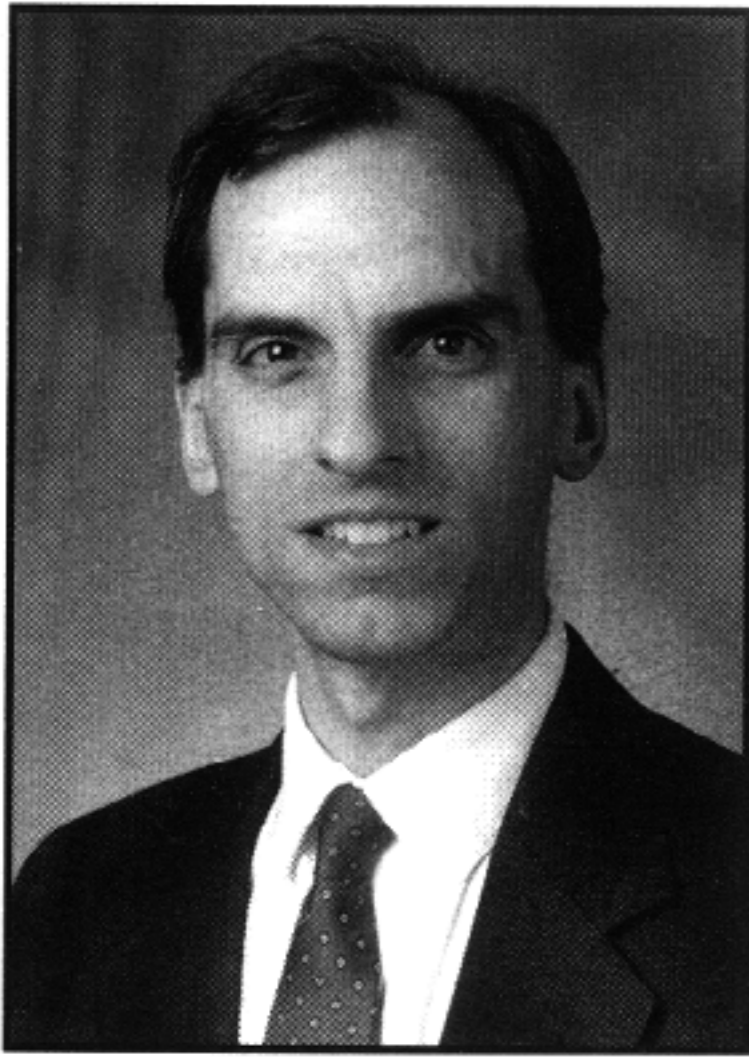
- Vol. 13, No. 24, pp. 729-730, Nov. 24, 1977.
7. P. A. J. Dupuis and C. K. Campbell, "Characteristic Impedance of Surface-Strip Coplanar Waveguides," *Elect. Lett.*, Vol. 9, No. 16, pp. 354-355, August 9, 1973.
8. G. Ghione and C. U. Naldi, "Coplanar Waveguides for MMIC Applications: Effect of Upper Shielding, Conductor Backing, Finite-Extent Ground Planes, and Line-to-Line Coupling," *IEEE Trans. Microwave Theory and Techniques*, Vol. MTT-35, No. 3, pp. 260-267, March 1987.
9. R. B. Marks, "A Multiline Method of Network Analyzer Calibration," *IEEE Trans. Microwave Theory and Techniques*, Vol. 39, No. 7, pp. 1205-1215, July 1991.
10. K. S. Yee, "Numerical Solution of Initial Boundary Value Problems Involving Maxwell's Equations in Isotropic Media," *IEEE Trans. Antennas Propagation*, Vol. 14, No. 3, pp. 302-307, May 1966.
11. S. Xiao, R. Vahldieck, "An Improved 2D-FDTD Algorithm for Hybrid Mode Analysis of Quasi-planar Transmission Lines," *1993 IEEE Int. Microwave Symp. Dig.*, Atlanta, Georgia, June 14-18, pp. 421-424, 1993.
12. G. Mur, "Absorbing Boundary Conditions for the Finite-Difference Approximation of the Time-Domain Electromagnetic-Field Equations," *IEEE Trans. Electromagnetic Compatibility*, Vol. 23, No. 4, pp. 377-382, Nov. 1981.
13. K. C. Gupta, R. Garg, and R. Chadha, *Computer-Aided Design of Microwave Circuits*, Artech House, Inc., Dedham, MA, 1981.
14. Y. C. Shih and T. Itoh, "Analysis of Conductor-Backed Coplanar Waveguide," *Elect. Lett.*, Vol. 18, No. 12, pp. 538-540, June 1982.

## About the Authors



Emmanouil M. Tentzeris was born in Piraeus, Greece, in 1970. Mr. Tentzeris received his Electrical Engineering and Computer Science degree from the National Technical University of Athens (NTUA), Athens, Greece, (Suma Cum Laude) in 1992. In 1993 Mr. Tentzeris received his M.Sc. degree from the University of Michigan, Ann Arbor, Michigan. Mr. Tentzeris is currently pursuing a Ph.D. degree at the University of Michigan. Since 1992, Mr. Tentzeris has been a Graduate Research Assistant at the Radiation Laboratory, University of Michigan. His research interests include the development of novel numerical techniques and the application of the principles of Multiresolution Analysis for the simulation of microwave circuits used in wireless or satellite communication system. Mr. Tentzeris is a member of the Technical chamber of Greece.





George E. Ponchak received his B.E.E. degree from Cleveland State University in 1983, the M.S.E.E. degree from Case Western Reserve University in 1987, and Ph.D. degree from the University of Michigan in 1997. In July 1983, he joined the staff of NASA Lewis Research Center in Cleveland, Ohio where he is a member of the Communication Technology Division. Since then, he has been interested in the development

and characterization of microwave and millimeter-wave printed transmission lines and passive circuits, multilayer interconnects, dielectric waveguides, uniplanar circuits, and microwave packaging. He has been responsible for the technical management of GaAs, InP, and SiGe grants and contracts. In addition, he is interested in the reliability of GaAs and SiGe MMICs for space applications. He is the author and co-author of more than 30 papers in referred journals and symposia proceedings. Dr. Ponchak is a member of the IEEE MTT-S and The International Microelectronics and Packaging Society (IMAPS).



Linda P.B. Katechi is a professor of E.E.C.S. and a Fellow of IEEE. She received the B.S.E.E degree from the National Technical University of Athens, Greece, in 1977 and the M.S.E.E. and Ph.D. degrees from the University of California, Los Angeles, in 1981 and 1984, respectively. In September 1984, she joined the faculty of the EECS Department of the University of Michigan, Ann Arbor. Since then, she has

been interested in the development and characterization (theoretical and experimental) of microwave, millimeter printed circuits, the computer aided design of VLSI interconnects, the development and characterization of micromachined circuits for millimeter wave and submillimeter wave applications and the development of low-loss lines for Terahertz-frequency applications. She has also been studying theoretically an experimentally various types of uniplanar radiating structures for hybrid-monolithic and monolithic oscillator and mixer designs. She has been awarded with the IEEE AP-S W.P. King (Best Paper Award for a Young Engineer) in 1984, the IEEE AP-S S.A. Schelkunoff Award (Best Paper Award) in 1985, the NSF Presidential Young Investigator award and an URSI Young Scientist Fellowship in 1987, the Humboldt Research Award and the University of Michigan Faculty Recognition Award in 1994 and the IEEE MTT-S Microwave Prize in 1996. She is a member of IEEE AP-S, MTT-S, Sigma XI, IMAPS Society, URSI Commission D and a member of AP-S ADCOM from 1992 to 1995. Also, she is serving as an associate Editor for the IEEE Transactions MTT-S.